**Proceedings of the 7th GACM Colloquium on Computational Mechanics
for Young Scientists from Academia and Industry
October 11-13, 2017 in Stuttgart, Germany**

Combined Macro- and Micro-Mechanical Analysis of Instable Crack Propagation in Interlaminar Fracture Toughness Tests

Michael Schober[1]*, Jörg Hohe[2] and Takashi Kuboki[3]

Micro Abstract
Fracture toughness experiments with fiber reinforced polymers often show instable growths of the observed cracks. Such discontinuities can occur as a result of the test specimen's microstructure. A combined macromechanical micromechanical simulation approach shall help understanding the occurrence of discontinuities with respect to the specimen's microstructure. Therefore, the fracture toughness test specimen's microstructure is analyzed and modeled for finite element analyses.

[1]Institute for Applied Materials - Computational Materials Science, Karlsruhe Institute of Technology, Karlsruhe, Germany

[2]Component Safety and Lightweight Construction, Fraunhofer Institute for Mechanics of Materials IWM, Freiburg, Germany

[3]Department of Mechanical and Materials Engineering, University of Western Ontario, London, Ontario, Canada

* **Corresponding author**: michael.schober@kit.edu

1 Introduction

Consolidated continuous fiber reinforced thermoplastic tapes have recently been used for light-weight structural parts as well as light-weight patching material to locally reinforce a specific part area [3]. The manufacturing process of consolidated tapes consists of three steps: tape laying, heating, and compression of the tape layers. It is important to understand how this manufacturing method affects interface microstructures and their mechanical properties, in particular, delamination fracture toughness between the tape layers. However, fracture toughness experiments rely on the measurement accuracy of a propagating crack, which can be difficult due to several reasons [1, 2]. Furthermore, stepwise and abrupt crack propagation can occur, making its evaluation regarding critical energy release rates imprecise. Considering microstructure investigations, a combined macro-micro-mechanical simulation approach shall help evaluate such vague results.

2 Sample Manufacturing and Testing

The manufacturing of the test material used industrial scale process equipment: an automated tape laying machine, a convection oven, and an hydraulic press. Continuous fiber reinforced tapes are cut, positioned and fixed to each other using the Fiberforge Relay 1000 (figure 1a). The semi-finished tape lay-up (figure 1b) is then heated up to a predefined temperature and compressed to its final shape, resulting in a consolidated plaque (figure 1c). A PTFE-foil creating an initial crack for oncoming fracture toughness tests is already placed during the tape laying process. Investigating the fracture toughness' sensitivity to process parameters, the consolidation temperature as well as the compression force has been varied in three levels from $260\,^\circ$C to $270\,^\circ$C and to $280\,^\circ$C and from 24 bar to 36 bar and to 48 bar, respectively, and analyzed fully factorial. The fracture toughness analysis is conducted with the *Double Cantilever Beam* (DCB) test for mode I fracture and with the *End Notched Flexure* (ENF) test for mode II fracture.

(a) Fiberforge Relay 1000 tape laying machine

(b) Tape lay-up including PTFE-foil

(c) Consolidated GF-PA6-plaque with PTFE-foil

Figure 1. Plaque manufacturing steps: automated tape laying machine (a), stacked tape lay-up (b), and the final, consolidated plaque (c)

The corresponding load-displacement curves are continuously recorded, while a camera system takes photos of the current specimen state periodically. Herewith, the crack propagation in the specimen is analyzed retrospectively. The critical energy release rates in mode I and mode II are computed with:

$$\mathcal{G}_{\mathbf{Ic}} = -\frac{\mathbf{d\Pi}}{\mathbf{dA}}, \qquad\qquad \mathcal{G}_{\mathbf{IIc}} = \frac{\mathbf{9 \times P \times a^2 \times d \times 1000}}{\mathbf{2 \times w\,(^1\!/_4 L^3 + 3a^3)}}, \tag{1}$$

where $\mathrm{d\Pi}$ is the dissipated energy over the crack area growth dA for $\mathcal{G}_{\mathrm{Ic}}$ [4], and where P is the critical load of 5 % stiffness degradation, d the crosshead displacement, w the specimen width, L the span length and a initial crack length for $\mathcal{G}_{\mathrm{IIc}}$, respectively. The experiments are conducted with a test rate of 2 mm/min for DCB tests and 1 mm/min for ENF tests.

3 Occurring Effects

The results of the fracture toughness analysis are shown in figure 2, where T1/P1 stands for the lowest temperature/pressure value and T3/P3 for the highest temperature/pressure value. In DCB tests, cracks propagate sequentially unstable and abrupt, as shown in figure 2(a) while stable crack growth can be rather rare. Therefore, the fracture toughness is evaluated in the surroundings of force drops. Both the DCB results and the ENF results in terms of the $\mathcal{G}_{\mathrm{Ic}}$ value and the $\mathcal{G}_{\mathrm{IIc}}$ value, respectively, scatter significantly. Process influence tendencies vanish within the computed standard deviation. Hence, drawing conclusions about the process sensitivity is

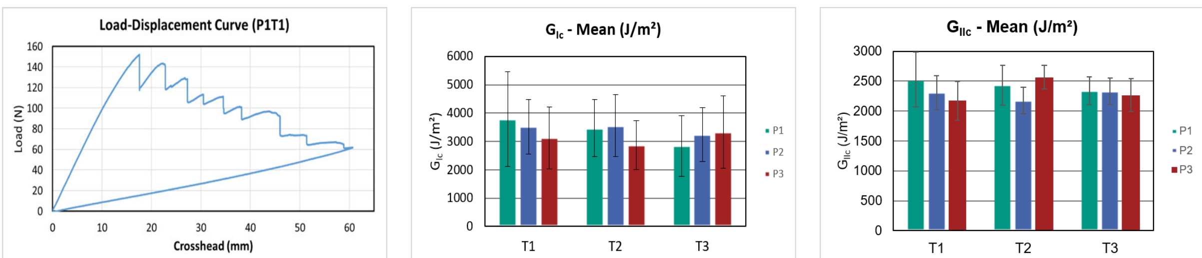

(a) Typical load-displacement curve (DCB)

(b) Results DCB tests

(c) Results ENF tests

Figure 2. Results of the fracture toughness analysis - typical DCB load-displacement curve and computed critical energy release rates

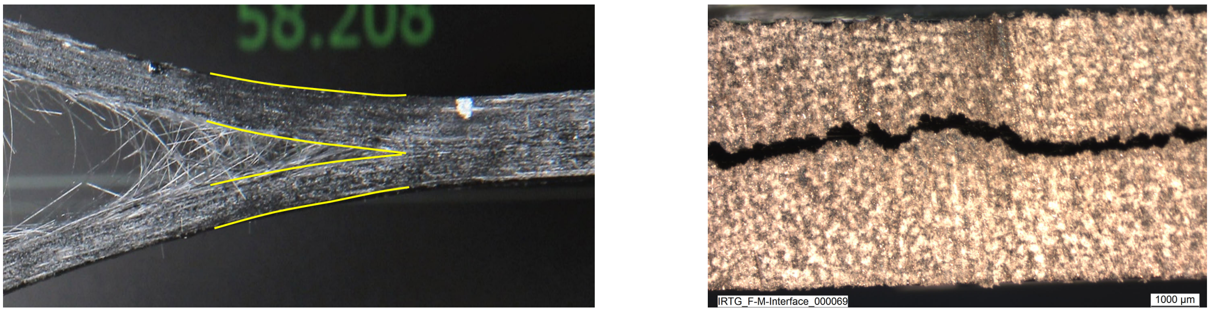

(a) Fiber bridging and asymmetric longitudinal crack path in DCB test

(b) Rough crack path in transverse direction

Figure 3. Fracture behavior of consolidated GF-PA6 tapes

hardly possible. Further investigation of the fracture behavior is therefore necessary. While cracks are propagating in DCB tests, several occurring effects are observable: as shown in figure 3(a), the crack crosses laminae while propagating, leading to major fiber bridging between the crack surfaces and an asymmetric crack path (as indicated with yellow lines). Furthermore, multiple cracks initiate concurrently.

4 Micromechanical and Numerical Analysis

Investigating the root causes of the crack behavior shown in figure 3, the fracture surface as well as the crack initiation area is analyzed using scanning electron microscopy. The SEM pictures of the fracture surface in figure 4(a) show exposed fiber surfaces next to free fiber beds within the plastically deformed matrix, indicating failure of the fiber matrix interfaces. Furthermore, ruptured fiber bundles and voids lead to a very rough fracture surface. The analysis of the specimens cross-section within the crack initiation area reveals, that first micro cracks initiate concurrently within fiber bundles, as shown exemplarily in figure 4(b), and then merge to form a macro crack. Although the fibers are well impregnated also in the densest bundles, the micro cracks mostly occur on or near the fiber matrix interfaces. This can be seen in particular between the fiber bundles, where the crack propagation is driven by growing cracks on the fiber matrix interfaces, where the matrix surrounding the fibers is still intact (figure 4(C)). Taking course from fiber bundle to fiber bundle, the cracks form the rough fracture surface seen in figure 3(b).

As the occurring effects and hence the results of the experiments are highly influenced by the materials microstructure, a numerical analysis considering the microstructural behavior in terms of fiber distribution and fiber bundling is conducted. Therefore, a combined macro-micro-mechanical approach is taken, where a sub-model for a statistical microstructure with a small

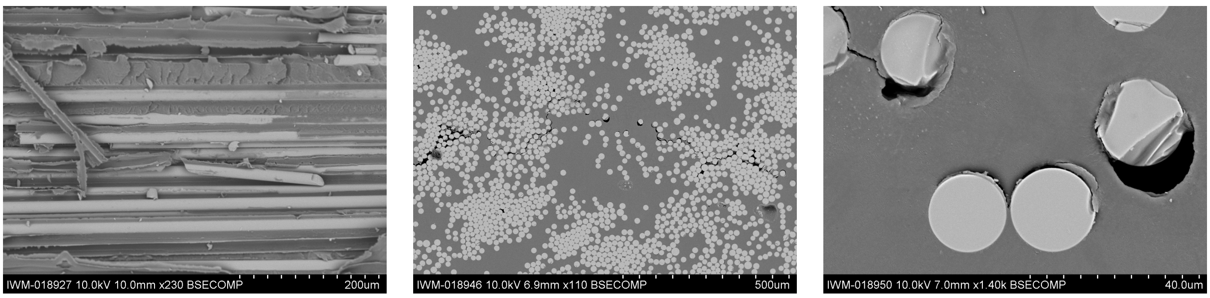

(a) Post-mortem fracture surface

(b) Initiating cracks in fiber bundles

(c) Failed interfaces between bundles

Figure 4. SEM-analysis of fracture behavior: cracks initiation and propagation is driven by fiber matrix interface failure

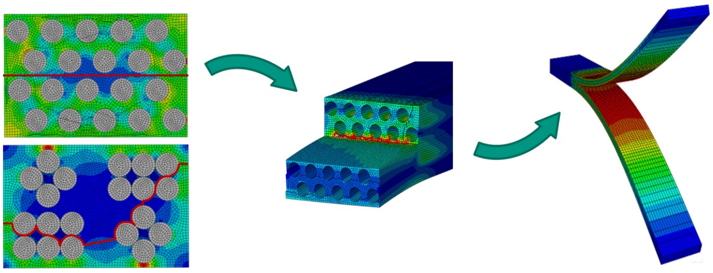

(a) Simulation approach using sub-models for microstructure effects

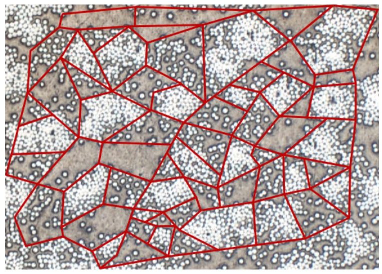

(b) Microstructure Voronoi clustering depending on fiber content

Figure 5. Macro-micro-mechanical simulation approach to reversely analyze fracture toughness experiments

number of fibers is embedded in a macromechanical model of a fracture toughness experiment, as shown in figure 5(a). Using a Voronoi procedure [5,6], this method can then be extended to a meso-scale considering the size, density and distribution of fiber bundles (figure 5(b)) and their effect on the crack propagation. Herewith, several possible micro-scale material properties, fiber distributions and crack paths can be analyzed to tghe fractographic observations in order to reversely identify interfacial strength and fracture toughness.

5 Conclusions

Fracture toughness experiments of FRP highly depend on the microstructural properties, which can lead to highly scattering and uncertain results. A combined macro-micro-mechanical analysis using numerical simulations can help evaluating a material's effective fracture behavior and its failure driving factors.

Acknowledgements

The research documented in this manuscript has been funded by the German Research Foundation (DFG) within the International Research Training Group **"Integrated engineering of continuous-discontinuous long fiber-reinforced polymer structures"** (GRK 2078).
The support by the German Research Foundation (DFG) is gratefully acknowledged.
The support by the company BASF in providing the raw material is gratefully acknowledged.
The composite work was performed at the Fraunhofer Project Centre (FPC) for Composite Research at the University of Western Ontario.

References

[1] J. H. Chen, E. Schulz, J. Bohse, and G. Hinrichsen. Effect of fibre content on the interlaminar fracture toughness of unidirectional glass-fibre/polyamide composite. *Composites Part A*, Vol. 30(6):p. 747–755, 1999.

[2] P. Davies and D. Moore. Glass/nylon-6.6 composites: delaminatin resistancs testing. *Composites Composites Science and Technology*, Vol. 38(3):p. 211–227, 1990.

[3] M. Graf. Verfahrenskombination für verschnittarmes ud-tapelegen. *Lightweight Design*, Vol. 9(1):p. 34–39, 2016.

[4] D. Gross and T. Seelig. *Bruchmechanik*. Springer Vieweg, 2016.

[5] V. Hardenacke and J. Hohe. Local stochastic analysis of the effective material response of disordered two-dimensional model foams. *PAMM*, Vol. 7(1):p. 4080001–4080002, 2007.

[6] V. Hardenacke and J. Hohe. Assessment of space division strategies for generation of adequate computational models for solid foams. *International Journal of Mechanical Sciences*, Vol. 52(12):p. 1772–1782, 2010.